Quantifying physical transport and local proliferation of phytoplankton downstream of an eutrophicated lake

Xinchen He[a,b], Hua Wang[a,b*], Lili Fan[a,b], Dongfang Liang[c], Yanhui Ao[a,b], Wei Zhuang[d]

[a] Key Laboratory of Integrated Regulation and Resource Development on Shallow Lake of Ministry of Education, College of Environment, Hohai University, Nanjing 210098, China

[b] College of Environment, Hohai University, Nanjing 210098, China;

[c] Department of Engineering, University of Cambridge, Cambridge CB2 1PZ, UK;

[d] Nanjing Institute of Environmental Sciences, MEP, Nanjing 210042, China;

*. Corresponding author's e-mail: wanghua543543@163.com.

Abstract: Eutrophication in a freshwater system has mainly been studied in lakes and their upstream rivers, which are responsible to bring pollutants into the lakes. However, the influence of lakes on downstream rivers suffered massive algae from upstream lakes has not been fully studied. Our study area is Liangxi river, downstream of Taihu Lake, which is highly eutrophicated. The algae in Liangxi river has two origins: the physical transport from Taihu Lake and the in-situ proliferation. This paper aims to apply numerical model to quantify these two processes. The model is calibrated against the measured data in 2018. This computational condition that includes both algal processes is termed as Scheme A. Then, we regarded phytoplankton as a conservative substance by turning off the phytoplankton biological process and calculated term it as Scheme E. We selected the chl-a concentration in Hongqiao (LX2) section to represent the amount of algae in Liangxi river. The average chl-a difference in this section between Schemes A and E, Δ_{ae}, can be used to quantify the magnitude of *in-situ* proliferation. The Δ_{ae} varies seasonally, and the annual average Δ_{ae} is 7.22 mg/m^3, which is 44.7% of the amount attributed to the physical transport. Liangxi river lies in an urban area which might encounter extreme events which to facilitate the *in-situ* proliferation, such as increased temperature and or excessive nutrient load. To quantify the level of algae under extreme situations, we design Schemes B, C and D which eliminated the limitation on algal growth by temperature, nitrogen and phosphorus respectively. Compared with the Scheme A, Schemes B, C and D oberve 21.8%, 65.7%and 61.2% respectively, increase in the average algal concentration. In the vertical direction, the chl-a concentration varies between 0.8mg/m³ and 2 mg/m³ in Scheme A, while the vertical concentration variances of chl-a in schemes B, C and D are found to be 5.56 mg/m³, 12.11 mg/m³ and 3.30 mg/m³, respectively.

Key word: Liangxi river; physical transport; in situ proliferation; numerical model

1.Introduction

Algal bloom is a serious problem threatening the health of aquatic ecosystem. The sewage with high nitrogen and phosphorus load caused by human activity, is released into the natural water, resulting in the unlimited growth of algae (Zhao et al., 2019). In the most freshwater ecosystem, the dominant phytoplankton community during algal bloom period were toxic cyanobacteria, such as *Microcystis aeruginosa* and *Aphanizomenon flos-aquae* (Major et al., 2018). These cyanobacterial species could release a type of hepatotoxin named microcystin. Long-term consuming water containing microcystin higher than 0.1μg/L (WHO, 2011) could induce a series of diseases including liver cancer (Lone et al., 2015). At present, most studies on controlling of algal bloom focus on shallow lakes (Pinardi et al., 2015; Simiyu et al., 2018; Xue et al., 2018), such as the cyanobacterial algal bloom in Lake Erie, America. In August 2014, the water supply to 600,000 people in Toledo was shut down for two days from Lake Erie (Steffen et al., 2017). Moreover, the algal bloom of Taihu Lake in 2007, caused the tap water contamination and made it undrinkable (Qin et al., 2010). Therefore, controlling of algal bloom is important and still needs to be studied.

There are many factors influencing the algal bloom, excessive nutrient load was commonly considered as one of the main environmental factors (McLean and Sinclair, 2012; Smith and Daniels, 2018). The cyanobacterial algal bloom which is especially dominated by *Microcystis aeruginosa*, *Anabaena flos-aquae* and *Aphanizomenon flos-aquae*, have excellent ability to absorb ambient N and P (Harke et al., 2016a) and gain a competitive advantage over the other phytoplankton. Some scholars have also proposed that rising temperature may be one of the causes of the bloom because cyanobacteria are thermophilic microbe with strong phototaxis, temperature increasing could provide a favorable temperature condition for cyanobacteria and induce the algal bloom (Harke et al., 2016b; Paul, 2008). However, in stream freshwater ecosystem, such as river, the vertical turbulence causes the gas vesicles of cyanobacteria to lose its function and thus weakens cyanobacterial ability to rise and receive light (Bukaveckas et al., 2018; Walsby and Bleything, 1988). So, compared with the ecosystem in those shallow and lentic lake, it is less possible for massive algal growth occur in rivers. However, the presence of in algal bloom rivers may have important implications for aquatic and even human health. For instance, the limitation factors of river algal bloom are still unclear. Phosphorus is considered as the limiting factors of lake algal bloom. But some researches about river algal bloom shows that the algal bloom still existed with reduction of phosphorus (Desortová and Punčochář, 2011; Hilton et al., 2006). Besides, each phytoplankton has a possible velocity range which is favorable for algal growth, while it is rarely considered in lake algal bloom. (Long et al., 2011) reported the most optimum flow velocity is 0.04m/s for dominant phytoplankton in Jaling river.

Lots on researches of river water quality focused on the upstream rivers of Taihu Lake, such as Wangyu river (Pan et al., 2015) and Xitiaoxi river(Lv et al., 2015). But for the outlets of Taihu Lake was few studied, such as our research area, Liangxi river. In recent decades, the urbanization surrounding the lake developed rapidly and the increasing human activities caused high nutrient load in Taihu Lake which triggered the expansion of the algal bloom (Hai et al., 2010; Ma et al., 2015), especially the northern Lake : Meiliang Bay, the most eutrophicated part of Taihu Lake (Wang et al., 2015). Liangxi river is the outlet of the Meiliang Bay. Since the outbreak of drinking water crisis in Wuxi city caused by algal bloom at Taihu Lake in 2007, the pump stations between Meiliang Bay and Liangxi river started working to accelerate the water circulation to improve the self-purification ability (Li et al., 2013; Maier et al., 2004). However, from the perspective of the water quality of Liangxi river, this measure also brought massive phytoplankton to it. Due to this, the odor from decayed phytoplankton threatened the health of riverside residents. The similar cases also occurred in other rivers, such as the Darling River, downstream of Menindee Lake, Australia (Mitrovic et al., 2011) and the upper James River, America (Qin and Jian, 2017). The overall retention time in Liangxi river is shorter comparing with rivers where algal bloom were reported. However, as an urban river, there are many stagnant zones in Liangxi river due to human control of hydrodynamic condition. The impact of stagnant regions is shown in a study of the tributaries of river Tames by (Bowes et al., 2012), who showed that the rivers that were connected to canal systems or lock systems had approximately six times higher chl-a concentrations than naturally flowing rivers of the same length. Thus, the size of the initial inoculum of phytoplankton is considered a key factor and the addition of impoundments to systems is likely to accelerate the development of phytoplankton (O'Hare et al., 2018). Furthermore, Liangxi river is also an urban river which suffered highly nutrient load from waste water, tributaries and urban runoff due to the development of urbanization in Wuxi city in recent decades. The local condition is suitable for algal growth and might change the phytoplankton community composition (Zhao et al., 2019). So, external algal input and *in-situ* proliferation, which one contributes more on algal distribution in Liangxi river? How much proportion did they each account? This requires more quantitively studies on eutrophication process in Liangxi river.

Our goal in this paper aims at: (1) developing a numerical hydrodynamic-eutrophication model of Liangxi river based on field investigating data in 2018. (2) carrying out numerical experiment to turn off the biological process of phytoplankton controlled only by physical transport, comparing the simulation results with that considering biological process to quantify the contribution of physical transport and *in-situ* proliferation on algal distribution in Liangxi river. (3) Turning off the temperature, nitrogen, phosphorus limitation on algal growth, to reveal the potential algal concentration in Liangxi river under excessive temperature or nutrient load and to calculate each factor’s limitation on *in-situ* algal growth.

2. Methods and Materials

2.1 Research area

Liangxi river is 7.97km in length, 20-25m in width and 2.66m in average depth. And it is also the primary river in Wuxi city river network, locates at the Northwest of Taihu Lake. Since 2007, the drinking water crisis happened in Wuxi city, the local government opened Meiliang and Duxuan Pump stations to transfer water from Taihu Lake to Liangxi river and finally into Beijing-Hangzhou Canal. The maximum of each pump station could reach $50m^3/s$. Liangxi river has 21 tributaries, which distribute in different district in Wuxi city. Due to massive algae in Liangxi river, the local government closed the gates between Liangxi river and tributaries to avoid the algal bloom expands. The current inflow to Liangxi river is mainly controlled by those two pump stations.

Liangxi river receives high nutrient load from urban human activities which could support phytoplankton to grow. According to the monitoring data by at Dushan section (Liangxi river) from 2010 to 2018 acquired from the website of the Wuxi hydrological Bureau (http://water.wuxi.gov.cn/), average ammonia concentration = 0.306mg/L, total phosphorus = 0.108 mg/L, TN = 1.906 mg/L. And the phytoplankton data of Meiliang Bay showed that the chl-a ranged from $20.97mg/m^3$ to $156.95mg/m^3$, and dominated by *Microcystis* and *Oscillatoria* (Li et al., 2015).

2.2 Field investigation

We investigated the geometry, water quality and hydrodynamic condition of Liangxi river in 2018. The geometry of Liangxi river and discharge of Meiliang and Daxuan pump stations was provided by Wuxi Hydrological Bureau. As for water quality observation, we selected biological oxygen demand, dissolved oxygen, nitrate, nitrite, phosphate, chlorophyll-a as our monitoring projects. The chl-a could represent phytoplankton biomass and was determined by spectrophotometer and the specific procedures refer to(Environment, 2017).

The other projects served as environmental factors influencing phytoplankton growth, including total nitrogen (TN), nitrite (NO_2^-), nitrate (NO_3^-), total phosphorus (TP), phosphate (PO_4^{3-}), dissolved oxygen (DO). TN was determined by Alkaline potassium persulfate digestion UV spectrophotometric method (Environment, 2012). NO_2^- was measured by Spectrophotometric method(Environment, 1987). The determination method of TP and PO_4^{3-} was Continuous flow analysis(CFA) and Ammonium molybdate spectrophotometry(Environment, 2013). As for DO measurement, we used the portable dissolved oxygen sensor (JPBJ-608) acquire data during sampling. . As for sampling strategy, we selected four typical sections in the river. LX1 is the junction of water from Meiliang and Daxuan pump stations. LX2 is one of the key sections of Jiangsu province and locates inside the urban area. LX3 is at the inlet of Mali river (the biggest tributary of Liangxi river). LX4 lies in the adjunction of Liangxi river and Beijing-Hangzhou Canal.

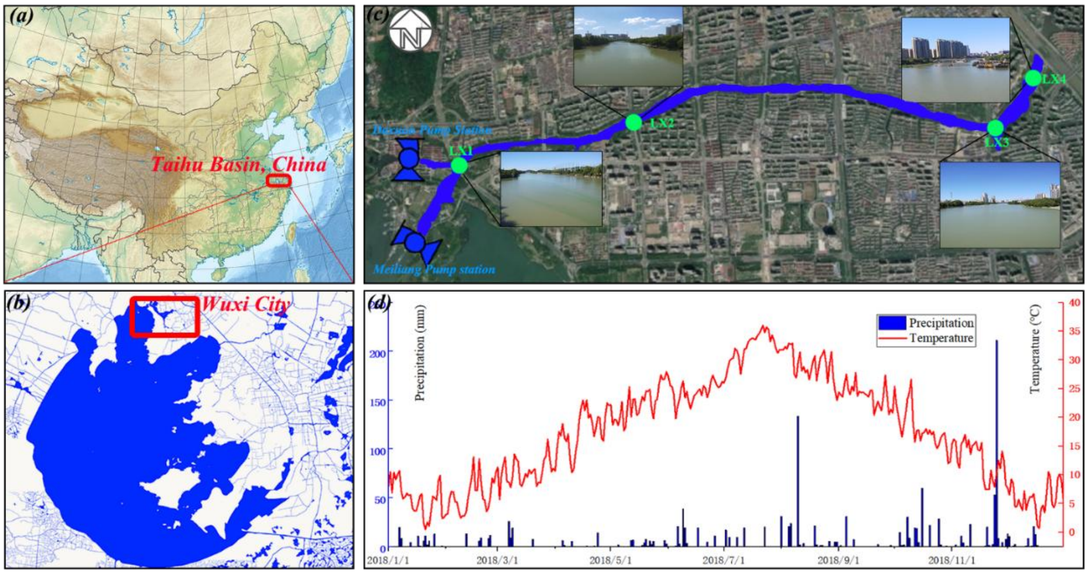

Fig.1 (a) Location of Taihu Basin. (b) Location of Liangxi river, Wuxi city. (c) Map of Liangxi river from Google Earth with sampling sites marked. (d) Temperature and precipitation of research area in 2018.

2.3 Numerical Experiment

2.3.1 Model Development

The DHI Mike 3 Flow model (FM) was applied to construct three-dimensional hydrodynamic model of Liangxi river. The computational grid was developed by Cartesian coordinates, and the sigma-coordinate transformation approach was used in the free surface. The computational mesh contained 1096 triangular elements and 3 vertical layers. The calculation time was between Jan 1st, 2018 to Dec 31st, 2018, and the timestep was set up with 60s.

- **Water Current Equation**

The model is based on numerical solution of three-dimensional incompressible Reynolds averaged Navier-Stokes equations invoking the assumptions of Boussinesq and of hydrostatic pressure (DHI, 2009b). The local continuity equation is written as

$$\frac{\partial u}{\partial x}+\frac{\partial v}{\partial x}+\frac{\partial w}{\partial x}=S\cdots\cdots\ (2.1)$$

And the momentum equations for x- and y- component, respectively

$$\frac{\partial u}{\partial t}+\frac{\partial u^2}{\partial x}+\frac{\partial vu}{\partial y}+\frac{\partial wu}{\partial z}=fv-g\frac{\partial \eta}{\partial x}-\frac{1}{\rho_0}\frac{\partial p_a}{\partial x}-\frac{g}{p_0}\int_z^n\frac{\partial \rho}{\partial x}dz-\frac{1}{\rho_0 h}\left(\frac{\partial s_{xx}}{\partial x}+\frac{\partial s_{xy}}{\partial y}\right)+F_u+\frac{\partial}{\partial x}\left(v_t\frac{\partial u}{\partial z}\right)+u_sS\cdots\cdots(2.2)$$

$$\frac{\partial v}{\partial t}+\frac{\partial v^2}{\partial y}+\frac{\partial uv}{\partial x}+\frac{\partial wv}{\partial z}=-fu-g\frac{\partial \eta}{\partial y}-\frac{1}{\rho_0}\frac{\partial p_a}{\partial y}-\frac{g}{p_0}\int_z^n\frac{\partial \rho}{\partial y}dz-\frac{1}{\rho_0 h}\left(\frac{\partial s_{yx}}{\partial x}+\frac{\partial s_{yy}}{\partial y}\right)+F_v+\frac{\partial}{\partial z}\left(v_t\frac{\partial v}{\partial z}\right)+v_sS\cdots\cdots(2.3)$$

In equation (2.1), (2.2) and (2.3), t is the time, x, y, z are the Cartesian co-ordinates; η is the surface elevation; d is the still water depth; h = η + d is the total water depth; u, v, w are the velocity components in the x, y and z direction. S_{xx}, S_{xy}, S_{yx} and S_{yy} are components of the radiation stress tensor; V_t is the vertical turbulent viscosity. The vertical viscosity was calculated by log-law formulation. Bed resistance and Smagorinsky coefficient were calibrate by velocity measurement of Liangxi river. The horizontal eddy viscosity was calculated by Smagorinsky formulation (Smagorinsky, 1963).

- **Transport Equation for a scalar quantity**

The conservation equation for a scalar quantity is given by

$$\frac{\partial C}{\partial t}+\frac{\partial uC}{\partial x}+\frac{\partial vC}{\partial y}+\frac{\partial wC}{\partial z}=F_C+\frac{\partial}{\partial z}\left(D_v\frac{\partial C}{\partial z}\right)-k_pC+C_SS\cdots\cdots(2.4)$$

Where C is the concentration of the scalar quantity, k_p is the linear decay rate of the scalar quantity, C_S is the concentration of the scalar quantity at the source and D_v is the vertical diffusion coefficient. F_C is the horizontal diffusion term defined by

$$F_C = \left[\frac{\partial}{\partial x}\left(D_h \frac{\partial}{\partial x} \right) + \frac{\partial}{\partial y}\left(D_h \frac{\partial}{\partial y} \right) \right] C \cdots\cdots (2.5)$$

where D_h is the horizontal diffusion coefficient.

- **Eutrophication Model**

The “Eutrophication Model 1” in Ecolab was applied to describe the eutrophication status in Liangxi river (DHI, 2009a). The fundamental principle of the eutrophication model is displayed by the flow charts in Fig.2. 12 variables are included in this model: phytoplankton carbon (PC), phytoplankton phosphorus, phytoplankton nitrogen (PN), chlorophyll-a (CH), zooplankton carbon (ZC), detritus carbon (DC), detritus nitrogen, detritus phosphorus (DP), inorganic nitrogen (IN), inorganic phosphorus (IP), dissolved oxygen (DO), benthic vegetation carbon (BC). Over 70 constants are included in the eutrophication model, and the DHI Mike Ecolab module has provided plausible range of each parameters. Since the Liangxi river originates from the Taihu Lake, which means both have similar biochemical characteristics and the dominant phytoplankton community is cyanobacteria, we could build the eutrophication model based on the previous laboratory tests and modelling studies of cyanobacteria in Taihu Lake. We used 14 representative parameters from their studies to build the eutrophication model, their values are presented in Table.1. For further accuracy of the model, we selected 5 sensitive parameters to calibrate and validate our model by monitoring results in LX1-LX4. According to (Huang et al., 2012), chl-a concentration in the model was sensitive to parameters related to algal growth (especially the P uptake) and loss (due to respiration). Thus we selected growth rate of phytoplankton, uptake of phytoplankton nitrogen, death of phytoplankton chlorophyll as parameters to calibrate the eutrophication model.

Table.1 List of Parameters in Hydrodynamic and Eutrophication Model

Parameters	Unit	Min	Max	Value	Reference
Growth rate phytoplankton	(/d)	0	2.5	1.8	Calibrate
Half-saturation constant for P uptake	g /m^3	0.001	0.05	0.015	Calibrate
Death of phytoplankton chlorophyll	g/m^3/d	0.05	0.27	0.15	Calibrate
Coefficient for max. chl-a production	1/(E/m^2/d)	1.1	1.9	1.1	(Mao et al., 2008)
Oxygen reaeration constant	(/d)	0	5.32	1.5	(Mao et al., 2008)
Temperature dependency growth rate	-	0.08	1.08	1.05	(Mao et al., 2008)
Light extinction constant phytoplankton	m^2/g	20	50	27	(Jiang et al., 2018)
Light extinction background constant	m^2	0.35	0.55	0.45	(Jiang et al., 2018)
Light extinction constant SS	m^2/g	0.1	1	0.25	(Jiang et al., 2018)
Sinking rate of phytoplankton	(m/d)	0.016	0.1728	0.086	(Huang et al., 2012)
Half-saturation constant for N uptake	g /m^3	0.1	0.6	0.14	(Ding et al., 2005)
intracellular concentration of N	mg/m^3	0.07	1.07	0.25	(Li et al., 2015)
intracellular concentration of P	mg/m^3	0.002	0.03	0.025	(Li et al., 2015)

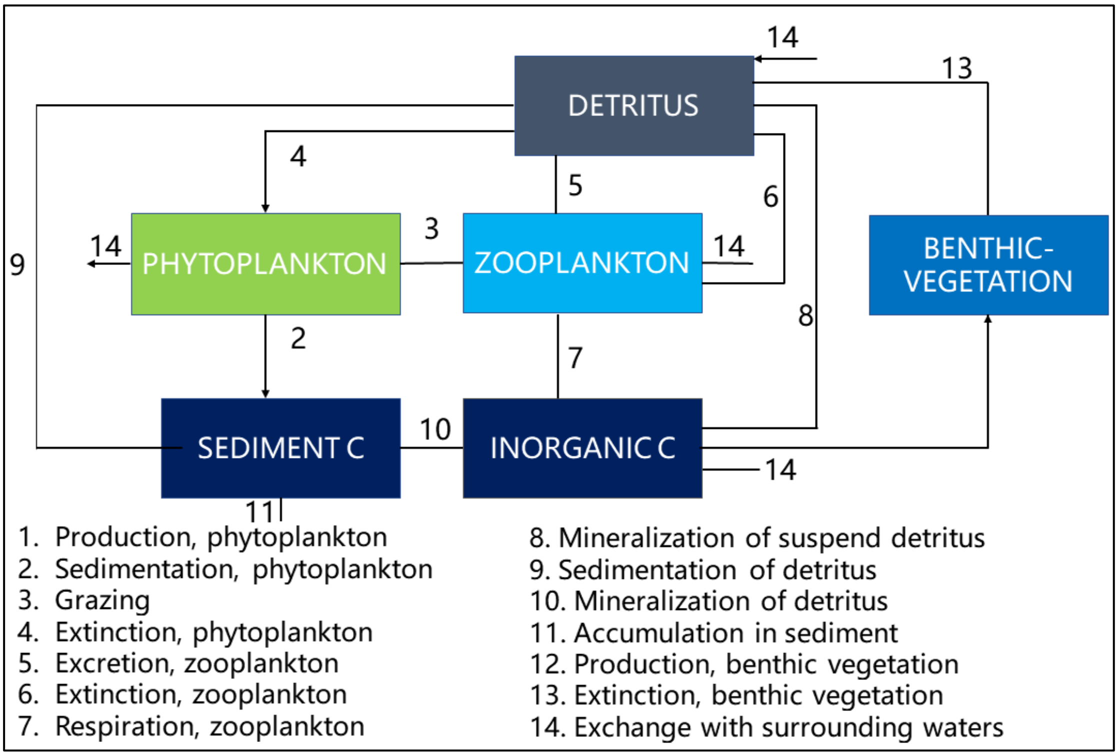

Fig.2 Simplified Flow Charts of Material Cycling in "Eutrophication Model 1"

2.3.2 Boundary Setting and Calculation Schemes

The Temperature and wind dataset are provided by China Meteorological Data Sharing Service System (http://cdc.cma.gov.cn:8081/home.do). The initial water quality condition was set as the spatial interpolation of measured data at in LX1, LX2, LX3, LX4 in

Jan 1st, 2018. The inflow boundary was set by the discharge data of Daxuan and Meiliang pump station. As Fig.3 shows, In 2018, Meiliang and Daxuan pumping station jointly transferred water to liangxi river, and the average daily water volume was 21.05 m^3/s.

We divided the year 2018 into three periods based on operation mode of the two pump stations. Period I: Daxuan pump station opened while Meiliang pump station closed. From Jan 1st to 5th (24.85m^3/s) and from Dec 22nd to 31st (20.45m^3/s). Period II: Meiliang Pump station on and Daxuan pump station off. From Jan 6th to 31st (19.41 m^3/s), Mar 20th to May 7th (21.16 m^3/s) and From Aug 25th to Dec 21st (21.43 m^3/s). Period III: the two pump stations run alternately and ensure the daily discharge to Liangxi river was around 20.64 m^3/s. From Feb 1st to Mar 19th (20.85 m^3/s), May 8th to Aug 24th (21.43 m^3/s).

At first, we input our geometry and hydrological (precipitation, discharge, water level) data to build the basic hydrodynamic model. Based on the calibrated hydrodynamic model, we add ecological part of chl-a which denotes the phytoplankton biomass into the model, then calibrated the model with chl-a monitoring data in 2018. The modeling results represents phytoplankton distribution under real situation (Scheme A). In order to separate the physical transport and local proliferation, we turned off the ecological process of chl-a and treated it as chemical substance, this modeling result represents the physical transport of algae (Scheme E). Temperature, light, nitrogen and phosphorus are considered as main impact factors on the *in-situ* proliferation. We designed 3 schemes (B, C, D) which turned off each factor's limitation respectively (Light was not separated in these schemes, since Liangxi river locates in urban area where the surrounding buildings will create variant covering effect in different time and that is hard to quantify.). The description of these 5 schemes were displayed in Table.2. For quantifying each factor's effect on *in-situ* proliferation, we defined a parameter: γ_i to represent each factors limitation.

$$\gamma_i = \frac{c_i - c_a}{c_i - c_e} \qquad i \in (b, c, d)$$

The c_a, c_b, c_c, c_d, c_e were calculation results of scheme A, B, C, D and E respectively. The larger the γ_i is, the greater the restriction degree of the ith factor on the algae growth (plan A) in actual situation. In another word, the potential risks on algal growth induced by the ith factor is greater.

Table.2 Calculation Schemes

Scheme	Description	Considering Limitation		
		Temperature	Nitrogen	Phosphorus
A	All Factors Considered	√	√	√
B	Elimination Temperature Limitation	-	√	√
C	Elimination of Nitrogen Limitation	√	-	√
D	Elimination of Phosphorus Limitation	√	√	-
E	Physical Transport	-	-	-

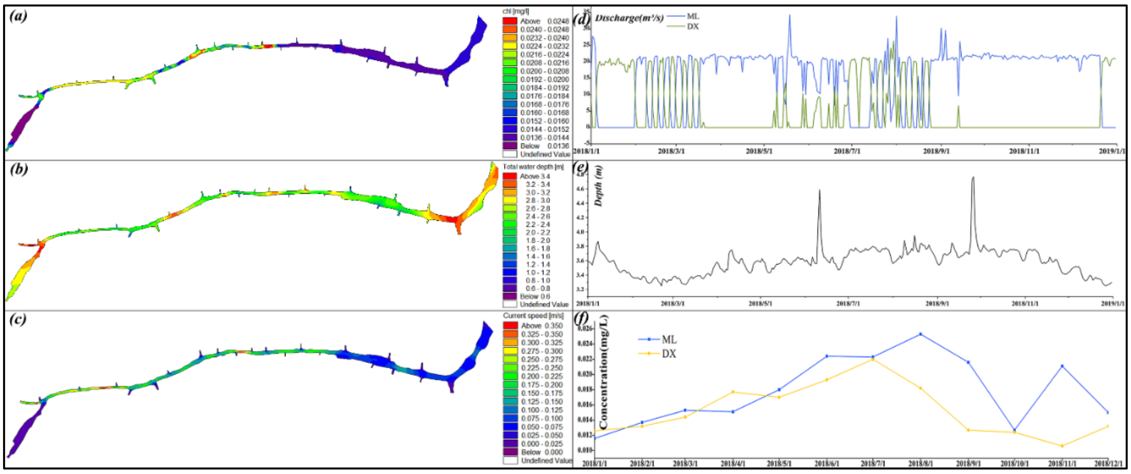

Fig.3 The thermal graph in (a), (b) and (c) showed the initial condition of chl-a , water depth and velocity; The daily discharge of Meiliang (ML) and Daxuan (DX) pump station was presented in (d) ; (e) is the curve of water level at the junction between the Liangxi river and the Bejing-Hangzhou Canal; (f) is the monthly chl-a concentration at the upstream of the two pump stations.

3. Results and Discussion

3.1 Model performance

Fig.4The model with algal biological process was calibrated and validated by the monitoring results in Liangxi river. In hydrodynamic part, the bed resistance was set as 0.05m. According to (Mangelsdorf et al., 1990), the bed resistance in a channel with unregulated rocks and benthic vegetation ranged from 0.040~0.067m. In ecological part of the model, through 60 times calculation of with 5 different values of phytoplankton growth rate, 4 different values of half-saturation constant for P uptake, 3 different values of death of phytoplankton chlorophyll. We found a set of these parameters which were 1.8 d^{-1}, 0.015 mg/L, 0.15 d^{-1} respectively. According to the parameters calibration results reported by (Huang et al., 2012), the phytoplankton grow rate was set as 1.145 d^{-1}. In the modelling study conducted by (Wang et al., 2017), it was assigned as 1.15 d^{-1}. However, based on the parameters sensitivity study of numerical model in Taihu Lake conducted by (Jiang et al., 2018), the algal growth rate was set as 2 d^{-1}. The growth rate of phytoplankton in our model was set as 1.8 d^{-1} which was in plausible range between previous modelling study of algal bloom in Taihu Lake. Phosphorus is reported as limiting factors for algal bloom in freshwater lakes (Hu et al., 2018; Wang et al., 2019). As a result, the half-saturation constant for P uptake were usually identified as sensitive parameters for algal models. (Mao et al., 2008) assigned this constant as 0.002 mg/L. According to (Ding et al., 2007), the half saturation constant for P uptake was set as 0.015mg/L, which is same value as our calibration result. Death of phytoplankton is the main method to control the loss of chl-a concentration, since our research area is a river channel and the flow disturbance would accelerate the phytoplankton death. So our calibration results of the phytoplankton death rate were relatively higher than other studies. For example, the death rate of phytoplankton was set as 0.10 d^{-1} by (Wang et al., 2017). The calculated results of chl-a were shown in Fig.4 indicated that the calculated value agree well with the field investigated data, and the relative errors at site LX3 and LX4 respectively ranged from 18.5%~19.6%. The model was capable of scientifically reflecting phytoplankton growth processes in Liangxi river.

According to the monitoring results, because of the river input was fully controlled by pump station and there was no tributary enter into Liangxi river, the daily calculation results in these sites shared an same fluctuation pattern. And the velocity variance depends on section width. The flowing velocity in LX2 ranged from 0.1-0.3 m/s with 42m the section width, and flowing velocity in LX4 ranged from 0.05-0.15m/s with 74m the section width. The chl-a calculation results all showed an pattern that higher in summer (June-September, 35 - 40 mg/m³) and lower in other seasons (20 -30 mg/m³).

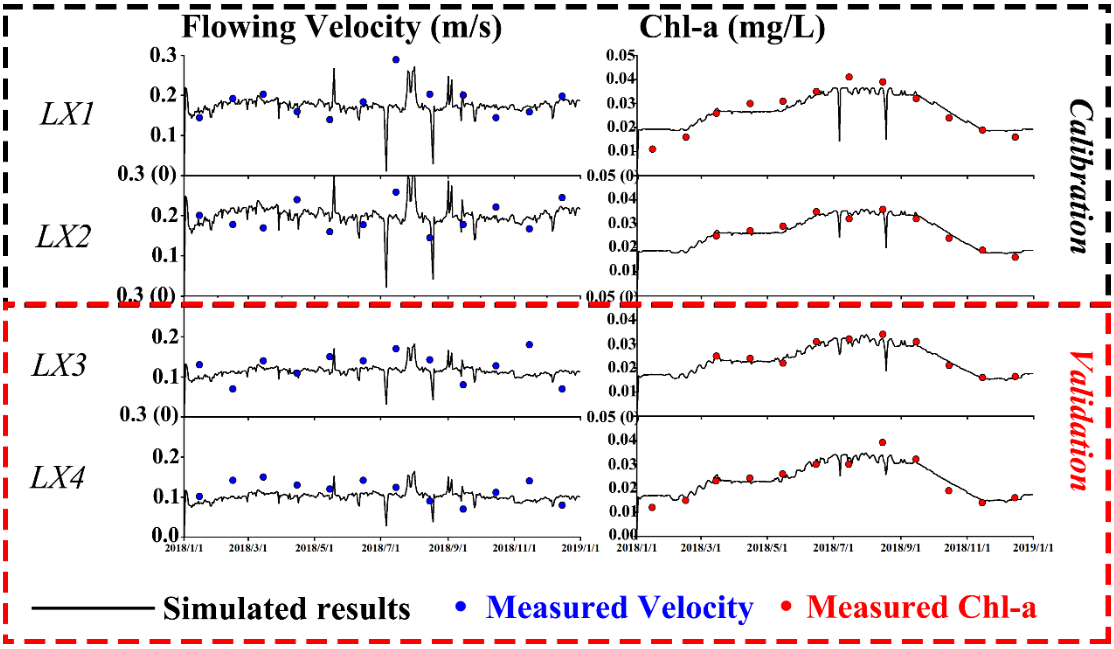

Fig.4 Calibration and Validation of simulated value in Liangxi River.

3.2 Separation of in situ Proliferation and Physical Transport

LX2, Hongqiao, located in the urban area of wuxi city, is one of the key section of Jiangsu province, which can be used as a typical section to represent the eutrophication condition of Liangxi river. The annual variation calculation results of the vertical average chl-a of Hongqiao section are shown in Fig.5. The correlation coefficient between calculation results of scheme A and E is 0.720 (p=0.000), indicating that the chl-a temporal variation pattern considered all factors was basically similar to that of physical transport. We could draw a conclusion that the temporal variation of chl-a in 2018 was mainly controlled by physical transport. Through comparison between curve A and E, we found: both calculation results of A and E stayed steady when pump stations operated isolated. Take results in January as an example, the chl-a concentration keep on 10 mg/m³ through physical transport but 23.19mg/m³ considering biological process. When the pumping station runs alternately, the result of chlorophyll-a in the corresponding scheme E also produces strong fluctuation. For instance, during 1st Feb to 15th March, which was recovery period of algae in Taihu Lake, both chl-a concentration in scheme A and E showed an increasing trend. However, the fluctuation of curve A is less than that of curve B. We deduced that is the zooplankton in scheme A model, the predator of phytoplankton, increasing its predation to the sudden rise of algal input to avert the sudden acceleration of algal biomass growth in Liangxi river. According to Fig.5, the annual difference value of scheme A and E is 7.22 mg/m³, which accounted for 41.7% of the annual average chl-a through physical transport.

Moreover, this difference value (Δ_{ae}) varied in different water transfer periods. In period I, Daxuan pump station on and Meiliang pump station off, Δ_{ae} ranged from 13.12 mg/m³. In period II, Meiliang pump station off and Daxuan pump station on, Δ_{ae} ranged from 2.0 ~ 4.4 mg/m³. In period III, two pump station ran alternately, Δ_{ae} varied from 2.0 m³ ~ 18.0 mg/m³. We could find that the *in-situ* proliferation of the algae in period I was 3.3~6.5 times larger than that in period II. The probable reason might be some algae tracked by the spiral flow field at LX1 in period I. As Fig.5 shows, because the elevation in north is larger than south(Gu, 2007), the water from Daxuan pump station in period I tend to flow down to the south and the pump force the water to go east, as Fig.6 shows, that created a clockwise helical flow and a portion of phytoplankton was trapped by this. However, the flow in other periods didn't showed that pattern. Thus, the substrate concentration in Liangxi river in period I is significantly smaller. Based on the growing curve of algae, low substrate algal concentration showed a higher ability to absorb nutrient and gain more chl-a increment (Fukuan et al., 2017).

The chl-a we discussed above mainly focus on vertical average concentration, since the vertical variance ranged from 0.8-2.0 mg/m³, which is negligible. However, it is still important to figure out the vertical distribution of algal *in-situ* growth. To analyze the vertical algal distribution in Hongqiao section, we selected chl-a in 5 typical days which could reflect chl-a distribution in different periods respectively as Fig.5 showed. And we divided the section horizontally into North (N, 14m from left bank), Central (C), and South (S, 14m from right bank). In vertical scale, we divided the section into Top layer (T, 1m from water), Middle layer (M), Bottom layer (B, 1m from bed). The section was separated into 9 regions as Fig.5 showed. And the vertical distribution patterns at each time could be described by Table.3. For instance, on Mar 3rd, which was in period III and spring (Temperature and light intensity was low). Algae in scheme A mainly assembled in NM region, in which chl-a concentration was 26.28mg/m^3. The general pattern of chl-a distribution is that in M > B > T, N > C > S. As for the calculation results of scheme E, the algae mainly concentrated in SM region (22.69mg/m^3), showed the pattern that chl-a in M > T> B, S > C > N. Based on the difference of vertical distribution pattern between scheme A and E, we could draw a conclusion that the *in-situ* proliferation contributed to vertical variance, which varied in different water transfer periods and seasons.

The Liangxi river is shallow and its flow regime is easy to be influenced. The pump station transferring water from Taihu Lake might induce the vertical disturbance. Besides, the wind impact (Stokes drift) might change the algae migration (Constantin, 2006; Wang et al., 2016). The vertical turbulence intensity increasing could accelerate the algae mixture in vertical scale and impair the buoyancy of phytoplankton (Liu et al., 2017). It can be seen from the chl-a distribution in schemes A and E that the vertical difference value ranged from 0.8 mg/m^3 ~2 mg/m^3, which was small vertical variance. However, the difference still existed and that was different in scheme A and E. That difference means *in-situ* proliferation might changed the vertical distribution pattern. The algae in scheme A possessed with phototaxis, thermotaxis and trophotropism would migrate to the favorable region (Coles and Jones, 2000; Mineeva and Mukhutdinov, 2018; Yang et al., 2012). In the vertical distribution thermal diagram in Fig.5, scheme E represented the algal distribution dominated by vertical turbulence, while scheme A denoted that was dominated by both vertical turbulence and *in-situ* proliferation of algae. We found that the vertical distribution of algae in schemes A and E did not gather in the surface water flow during the non-algal bloom period, possibly because the rapid surface water flow inhibited the algal growth and assemblage (Huang et al., 2016). It is also possible that wind disturbances caused the algae on the surface to sink faster. In algal bloom period which was during June to September. According to scheme E results in 2018/8/25, under the effect of the vertical turbulence caused by alternately water transferring, the algae concentrated at the middle layer. However, in scheme A, algae with biological properties tended to spread to top layer. This might attribute to the phototaxis and thermotaxis.

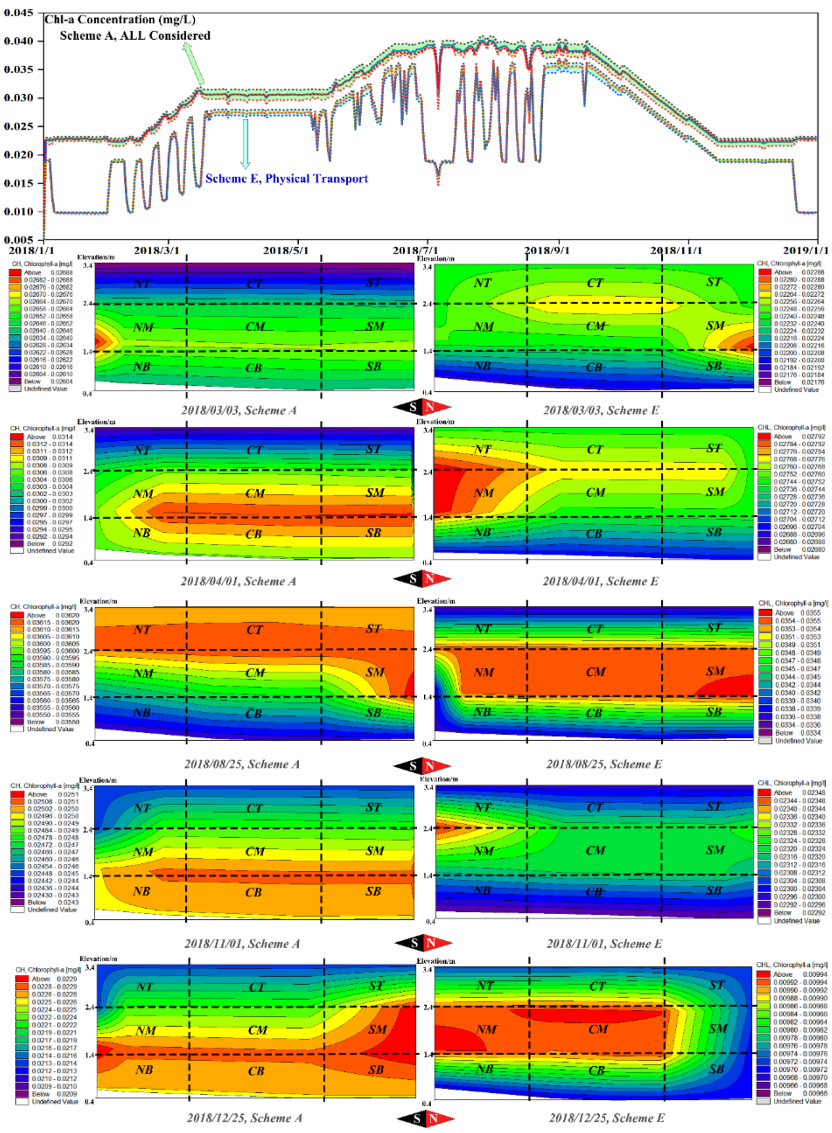

Fig.5 Upper curve denotes the chl-a calculation results of scheme A and E in Hongqiao station (LX2). The solid line represents the average chl-a section, the black dotted line represents the concentration of chl-a in the surface water, the red dotted line represents the concentration of chl-a in the middle water, and the blue dotted line represents the concentration of chl-a in the bottom water. The thermal charts below represent the vertical distribution of chl-a

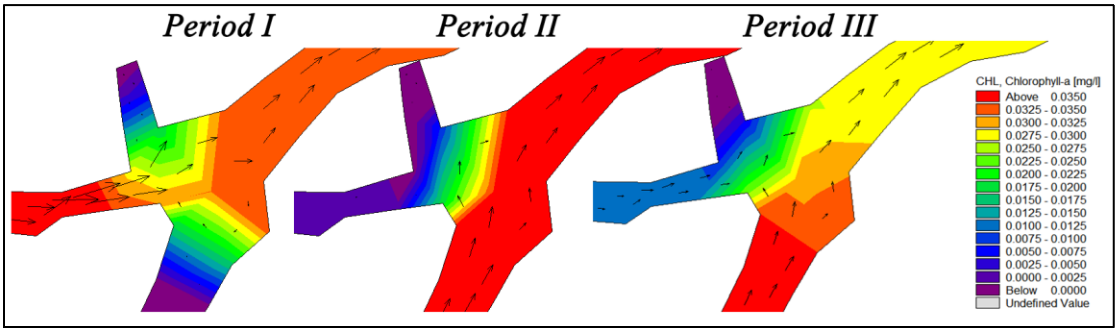

Fig.6 The flow direction at LX1 in different water transfer period

Table.3 Chl-a Vertical Distribution at LX2 Calculated by Scheme A and E

Time	Period	Scheme	Concentrated Regions	Distribution Pattern
2018/3/3	III, Spring	A	NM (26.28mg/m³)	M > T> B, S > C > N
		E	SM (22.69mg/m³)	M > T> B, S > C > N
2018/4/1	II, Spring	A	CM (31.10 mg/m³), SM (31.11 mg/m³)	M > T > B, S > C >N
		E	NM (27.70 mg/m³), NT (27.48 mg/m³)	M > T > B, N > C > B
2018/8/25	III, Summer	A	ST (36.15 mg/m³) CT (36.15 mg/m³)	T > M > B, S > C > N
		E	SM (35.55 mg/m³) CM (35.55 mg/m³)	M > T> B, S > C > N
2018/11/1	II, Fall	A	SB (25.02 mg/m³) CB (25.02 mg/m³)	B > M > T, N > C > S
		E	NM (23.40 mg/m³) NT (23.48 mg/m³)	M > T > B, N > C > S
2018/12/25	I, Winter	A	SM (22.65mg/m³)	B > M > T, S > C> N
		E	SM (9.94 mg/m³) CM (9.94 mg/m³)	M > T > B, N > C > S

3.3 Potential Algal Concentration Under Rising Temperature and Excessive Nutrient

Nutrients and temperature are regarded as the main factors limiting algal growth. To quantify each limiting effect on algal *in-situ* proliferation, we set 3 schemes (Scheme B, C, D) which eliminated temperature, nitrogen and phosphorus effect on algal growth respectively. On the other hand, the calculation results of these schemes could also represent the potential chl-a concentration in Liangxi river under rising temperature or excessive load in river. The calculation results and the limitation degree (γ_i) were shown in Fig.7 including chl-a concentration in the top, middle and bottom layer. In scheme B, we eliminated the temperature effect, which also means the seasonal influence was eliminated. But chl-a concentration in scheme B still showed a similar temporal pattern with that in scheme A: higher in summer and lower in other seasons. We could draw a conclusion that the temporal pattern in chl-a concentration in scheme A was mainly controlled by the inoculum of algae, rather than the algal growth in Liangxi river. However, eliminating these limiting effects did facilitate the algal growth. In scheme B, the maximum of chl-a reached 65.0 mg/m³, and the annual average concentration has increased 21.8% comparing with chl-a concentration in scheme A. The annual average of the temperature limitation parameter (γ_b) on algal growth was 0.368. In scheme C, when nitrogen limitation on algal growth was removed, the maximum chl-a concentration could reach 64.9 mg/m³, the annual average chl-a concentration increased 65.7% from that in scheme A. The annual average of the nitrogen limitation parameter (γ_c) on algal growth was 0.623. In scheme D, phosphorus limitation was eliminated, the maximum chl-a concentration was up to 62.2 mg/m³, annual average chl-a increased by 61.2% relative to that in scheme A. The annual average of the phosphorus limitation parameter (γ_b) on algal growth was 0.580.

By comparing the chl-a concentration under different extreme events, we found the potential algal concentration increment induced by climate warming was less than that induced by excessive nutrient load. Averagely speaking, the temperature limitation effect on algal growth was less than the nutrient limitation. Although the global warming was reported to be main factor to trigger and expand algal bloom (Deng et al., 2016; Jatmiko et al., 2016; Manning and Nobles, 2017; Paul, 2008), the insufficient nutrient was not capable to support massive algal growth induced by temperature rising. Through comparing nitrogen and phosphorus effect on algal growth, in real situation, the limitation effect of the latter on the growth of algae was less than the former. In other word, the potential algal concentration induced by excessive phosphorus might be less than by nitrogen. This was different with most researches on algal bloom control in other places, many researchers believe phosphorus was the main limiting factors on algal growth (Conley et al., 2009; Irie et al., 2018; Wurtsbaugh, 2015; Zeng et al., 2016). And controlling the exogenous phosphorus into the aquatic ecosystem was the most efficient way to limit algal growth. However, because Liangxi river received massive algal inoculum from the upstream, which also brings potential endogenous nutrient (PC, PN, PP). And that could serve as nutrient supplement and increased the buffer power to sustain phosphorus support (Zhu et al., 2013). Moreover, in algal bloom period, the phytoplankton dominated by cyanobacteria would accelerate the phosphorus releasing from the sediment. However, the research about estimating the TN and TP load in Taihu Lake indicated that the amount of nitrogen releasing was less than that of phosphorus (Zhao et al., 2013). Therefore, controlling the input of exogenous nitrogen into the river may be more effective than controlling the inflow of phosphorus into the river.

Moreover, the vertical variance of chl-a concentration was also amplified when eliminating the effect of algal growth comparing with that in scheme A: The average vertical differences of scheme B, C and D through 2018 was 5.56 mg/m^3, 12.11 mg/m^3 and 3.30 mg/m^3 respectively (the average difference in scheme A was 1.2 mg/m^3). When nitrogen limitation removed, the algal concentration difference was largest among all the schemes. Which indicated the nitrogen impact on algal growth was the dominant factor on sustaining vertical homogeneity of chl-a concentration. Without nitrogen limitation, algae showed a distribution pattern : chl-a in top layer > middle layer > bottom layer. However, in real situation, the sediment will release inorganic nitrogen such as ammonia under the disturbance of the overlying water (Qin and Hu, 2018). Besides, the nitrogen fixing reaction at the surface layer was anaerobic. High dissolved oxygen inhibited that reaction at the top layer. Thus, the inorganic nitrogen was less than that at the bottom layer (Paerl, 2017). In order to acquire more inorganic nitrogen, the phytoplankton might have a tendency to sink down. But the vertical difference of each scheme shows different patterns. Chl-a in scheme B and C showed that the concentration in the top layer > middle layer > bottom layer. In these two schemes, c(T) – c(M), which was the chl-a concentration difference between top layer and middle layer, basically equaled to the value of c(M) – c(B), which was the chl-a difference value between middle layer and bottom layer. However, in scheme D, chl-a concentration in middle layer was higher than that in top and bottom layer from July to September, lower in the other months. In our model, the phosphorus input was the sum of mineralization of detritus, phytoplankton, zooplankton and the release from sediment(Prentice et al., 2019). The mineralization would decrease with increased depth, and the phosphorus limitation effect in the middle layer would be greater than that in the top layer. However, the sediment in the bottom layer would support more phosphorus supply under the overlying water turbulence. Thus, the middle layer phosphorus limitation degree was greater than that in the top layer and the bottom layer. As the vertical distribution in scheme E on Aug 24th showed in Fig.5, the chl-a was supposed to gather in the middle layer only considering the physical transport. Thus, when phosphorus limitation was eliminated, the chl-a in the middle layer showed more potentials on algal growth.

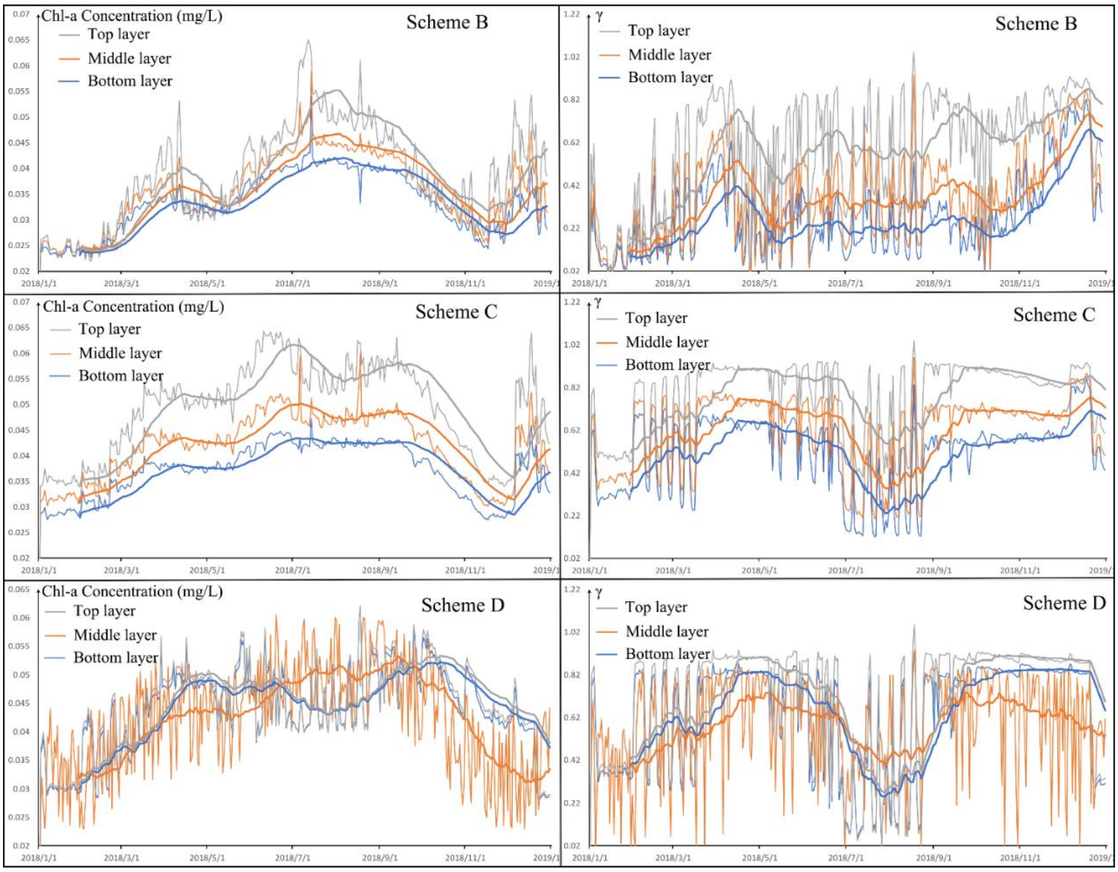

Fig.6 The left three charts showed the calculation results of scheme B, C and D. The three charts on the right was the calculation results of γ. The thicker lines in these charts are 30-day average of the calculation results.

4. Conclusions

In a lake-river system, the dynamic interaction between the lake and river can play a key role in hydro-environment. The Liangxi river receives massive algal input from the upstream Taihu Lake. Hence, there are two processes contributing to the algal concentration in Liangxi river: physical transport and *in-situ* proliferation. In this paper, we developed a numerical hydrodynamic-phytoplankton model to simulate the chl-a concentration evolution in Liangxi river, which was calibrated by field investigation data. In order to separate the physical transport and *in-situ* proliferation processes, we simulated the chl-a distribution due to the physical transport by turning off the biological process of the algae, which is termed as Scheme E. The model that considered both the physical transport and biological processes is named Scheme A. Through the results in Schemes A and E, we found that the temporal pattern of chl-a concentration largely depended on physical transport. The *in-situ* proliferation process exerted a smaller influence and its contribution relied on the season and the water transfer pattern at the two upstream pump stations. By comparing the chl-a change in LX2 in Schemes A and E, we found that the chl-a concentration fluctuated drastically when the two pump stations working alternatively. In scheme E, the buffer effect associated with the biological process led to a relatively small fluctuation of the chl-a concentration. Moreover, the difference in the chl-a vertical distribution in LX2 between Schemes A and E indicated that *in-situ* proliferation had an impact on vertical migration in such a highly turbulent river.

In-situ proliferation's impact on chl-a concentration is limited by temperature and availability of nutrients. We eliminated temperature, nitrogen and phosphorus limitations, respectively, in Schemes B, C and D. The results in these Schemes could represent the potential chl-a concentration under the extreme events such as extreme warming and excessive nutrient input. We introduced a parameter γ_i based on these results to quantify the temperature, nitrogen, phosphorus limitation effects on algal growth in Liangxi river. Comparing results in Schemes B, C and D, we found the different limitation factors on algal growth showed the following trend: temperature < phosphorus < nitrogen. Hence, the algal bloom in Liangxi river can be effectively avoided by controlling the nitrogen level. The pollutant releasing from sediment was not taken into consideration in this paper, which might influence the chl-a vertical distribution. We are going to take sample of river sediment next year and design an experiment to study the sediment releasing effect of Liangxi river. The experiment results are expected to be added into sediment module to make the model more accurate.

5. Acknowledge

This work was supported by the National Natural Science Foundation of China (No.51779075), A Project Funded by the Priority Academic Program Development of Jiangsu Higher Education Institutions, and the Major Science and Technology Program for Water Pollution Control and Treatment of China (2017ZX07203002-01). The authors express their thanks to Dr. Liu Zhiqi and Dr. Yan Yu for their help with data analysis.

References

Bowes, M.J. et al., 2012. Spatial and temporal changes in chlorophyll-a concentrations in the River Thames basin, UK: Are phosphorus concentrations beginning to limit phytoplankton biomass? Science of The Total Environment, 426: 45-55. DOI:https://doi.org/10.1016/j.scitotenv.2012.02.056

Bukaveckas, P.A., Franklin, R., Tassone, S., Trache, B., Egerton, T., 2018. Cyanobacteria and cyanotoxins at the river-estuarine transition. Harmful Algae, 76: 11-21. DOI:10.1016/j.hal.2018.04.012

Coles, J.F., Jones, R.C., 2000. Effect of temperature on photosynthesis-light response and growth of four phytoplankton species isolated from a tidal freshwater river. Journal of Phycology(1): 36.

Conley, D.J. et al., 2009. Ecology. Controlling eutrophication: nitrogen and phosphorus. Science, 323(5917): 1014.

Constantin, A., 2006. The trajectories of particles in Stokes waves. Inventiones Mathematicae, 166(3): 523-535.

Deng, J. et al., 2016. Phytoplankton assemblages respond differently to climate warming and eutrophication: A case study from Pyhäjärvi and Taihu. J. Gt. Lakes Res., 42(2): 386-396.

Desortová, B., Punčochář, P., 2011. Variability of phytoplankton biomass in a lowland river: Response to climate conditions. Limnologica, 41(3): 0-166. DOI:https://doi.org/10.1016/j.limno.2010.08.002

DHI, 2009a. MIKE 3 Flow Model, ECO Lab Module, User Guide.

DHI, 2009b. MIKE 3 Flow Model, Hydrodynamic Module, Scientific Documentation.

Ding, L. et al., 2007. Simulation study on algal dynamics based on ecological flume experiment in Taihu Lake, China. Ecological Engineering, 31(3): 200-206. DOI:https://doi.org/10.1016/j.ecoleng.2007.06.013

Environment, Minisitry of Ecological Environment., 1987. Water quality - Determination of nitrogen (nitrite) - Spectrophotometric method China.

Environment, Minisitry of Ecological Environment., 2012. Water Quality Determination of total nitrogen- Alkline potassium persulfate digestion UV spectrometrophotometric method China.

Environment, Minisitry of Ecological Environment., 2013. Water quality-Determination of orthophosphate and total phosphorus-Continuous flow analysis(CFA) and Ammonium molybdate spectrophotometry, China.

Environment, Minisitry of Ecological Environment., 2017. Water quality—Determination of chlorophyll a—Spectrophotometric method, China.

Fukuan, L.I., Zheng, J., Jia, Z., Sun, L., 2017. Impact of Nitrogen and Phosphorus on algal growth and kinetics in Haihe River of Tianjin. Chinese Journal of Environmental Engineering, 11(2): 959-964.

Gu, Y., 2007. Iteration searching algorithm of transition from regular DEM terrain data to TIN model. Computer Engineering & Applications, 43(23): 69-71.

Hai, X.U. et al., 2010. Nitrogen and phosphorus inputs control phytoplankton growth in eutrophic Lake Taihu, China. Limnology & Oceanography, 55(1): 420-432.

Harke, M.J., Davis, T.W., Watson, S.B., Gobler, C.J., 2016a. Nutrient-Controlled Niche Differentiation of Western Lake Erie Cyanobacterial Populations Revealed via Metatranscriptomic Surveys. Environmental Science & Technology, 50(2): 604-615. DOI:10.1021/acs.est.5b03931

Harke, M.J. et al., 2016b. A review of the global ecology, genomics, and biogeography of the toxic cyanobacterium, Microcystis spp. Harmful Algae, 54: 4-20. DOI:https://doi.org/10.1016/j.hal.2015.12.007

He, G. et al., 2011. Application of a three-dimensional eutrophication model for the Beijing Guanting Reservoir, China. Ecological Modelling, 222(8): 1491-1501. DOI:10.1016/j.ecolmodel.2010.12.006

Hilton, J., O'Hare, M., Bowes, M.J., Jones, J.I., 2006. How green is my river? A new paradigm of eutrophication in rivers. Science of The Total Environment, 365(1): 66-83. DOI:https://doi.org/10.1016/j.scitotenv.2006.02.055

Hu, X. et al., 2018. Monitoring and research of microcystins and environmental factors in a typical artificial freshwater aquaculture pond. Environ Sci Pollut Res Int, 25(6): 5921-5933. DOI:10.1007/s11356-017-0956-4

Huang, J., Gao, J., Hörmann, G., 2012. Hydrodynamic-phytoplankton model for short-term forecasts of phytoplankton in Lake Taihu, China. Limnologica, 42(1): 7-18.

Huang, J. et al., 2016. Experiment study of the effects of hydrodynamic disturbance on the interaction between the cyanobacterial growth and the nutrients. Journal of Hydrodynamics, 28(03): 411-422.

Irie, M., Hirose, F., Okada, T., Mattern, J.P., Fennel, K., 2018. Modeling of nitrogen and phosphorus profiles in sediment of Osaka Bay, Japan with parameter optimization using the polynomial chaos expansion. Coastal Engineering Journal, 60(4): 499-515.

Jatmiko, W. et al., 2016. Algal growth rate modeling and prediction optimization using incorporation of MLP and CPSO algorithm, International Symposium on Micro-nanomechatronics & Human Science.

Jiang, L. et al., 2018. Parameter uncertainty and sensitivity analysis of water quality model in Lake Taihu, China. Ecological Modelling, 375: 1-12. DOI:10.1016/j.ecolmodel.2018.02.014

Li, Y. et al., 2013. Improved Yangtze River Diversions: Are they helping to solve algal bloom problems in Lake Taihu, China?, 51, 104–116 pp. DOI:10.1016/j.ecoleng.2012.12.077

Li, Z., Chen, Q., Xu, Q., 2015. Modeling algae dynamics in Meiliang Bay of Taihu Lake and parameter sensitivity analysis. Journal of Hydro-environment Research, 9(2): 216-225. DOI:https://doi.org/10.1016/j.jher.2014.10.001

Liu, F., Zeng, L., Wu, Y.H., Baoligao, B., Chen, X., 2017. Vertical distribution of motile phytoplankton in density currents, Iop Conference Series: Earth & Environmental Science.

Lone, Y., Koiri, R.K., Bhide, M., 2015. An overview of the toxic effect of potential human carcinogen Microcystin-LR on testis. Toxicology Reports, 2: 289-296.

Long, T.Y., Wu, L., Meng, G.-h., Guo, W.-h., 2011. Numerical simulation for impacts of hydrodynamic conditions on algae growth in Chongqing Section of Jialing River, China. Ecological Modelling, 222(1): 112-119.

Lv, H., Xu, Y., Han, L., Zhou, F., 2015. Scale-dependence effects of landscape on seasonal water quality in Xitiaoxi catchment of Taihu Basin, China. Water Science & Technology A Journal of the International Association on Water Pollution Research, 71(1): 59-66.

Ma, J. et al., 2015. Controlling cyanobacterial blooms by managing nutrient ratio and limitation in a large hypereutrophic lake: Lake Taihu, China. Journal of Environmental Sciences, 27(01): 80-86. DOI:79a2e37cdcb4dea042abe9191041d7dd

Maier, H., Humphrey, G., Clark, T., Frazer, A., Sanderson, A., 2004. Risk- based approach for assessing the effectiveness of flow management in controlling cyanobacterial blooms in rivers, 20, 459-471 pp. DOI:10.1002/rra.760

Major, Y., Kifle, D., Spoof, L., Meriluoto, J., 2018. Cyanobacteria and microcystins in Koka reservoir (Ethiopia). Environmental Science and Pollution Research, 25(27): 26861-26873. DOI:10.1007/s11356-018-2727-2

Mangelsdorf, J., Scheurmann, P.D.-I.K., Weiß, F.H., 1990. Hydraulics of Stream Flow. Springer Berlin Heidelberg.

Manning, S.R., Nobles, D.R., 2017. Impact of Global Warming on Water Toxicity: Cyanotoxins. Current Opinion in Food Science, 18.

Mao, J., Chen, Q., Chen, Y., 2008. Three-dimensional eutrophication model and application to Taihu Lake, China. Journal of environmental sciences (China), 20(3): 278-84. DOI:10.1016/S1001-0742(08)60044-3

McLean, T.I., Sinclair, G.A., 2012. Harmful Algal Bloomsharmful algal bloom (HAB). In: Meyers, R.A. (Ed.), Encyclopedia of Sustainability Science and Technology. Springer New York, New York, NY, pp. 4819-4846. DOI:10.1007/978-1-4419-0851-3_829

Mineeva, N.M., Mukhutdinov, V.F., 2018. Vertical Distribution of Chlorophyll in the Upper Volga Reservoirs. Inland Water Biology, 11(1): 13-20.

Mitrovic, S.M., Hardwick, L., Dorani, F., 2011. Use of flow management to mitigate cyanobacterial blooms in the Lower Darling River, Australia. Journal of Plankton Research, 33(2): 229-241.

O'Hare, M. et al., 2018. Responses of Aquatic Plants to Eutrophication in Rivers: A Revised Conceptual Model. Frontiers in Plant Science, 9. DOI:10.3389/fpls.2018.00451

Paerl, H., 2017. The cyanobacterial nitrogen fixation paradox in natural waters. F1000research, 6(6): 244.

Pan, X.X., Ying-Qun, M.A., Qin, Y.W., Zou, H., 2015. Nutrients Input Characteristics of the Yangtze River and Wangyu River During the “Water Transfers on Lake Taihu from the Yangtze River”. Environmental Science, 36(8): 2800.

Paul, V.J., 2008. Global warming and cyanobacterial harmful algal blooms. In: Hudnell, H.K. (Ed.), Cyanobacterial Harmful Algal Blooms: State of the Science and Research Needs. Springer New York, New York, NY, pp. 239-257. DOI:10.1007/978-0-387-75865-7_11

Pinardi, M. et al., 2015. Assessing Potential Algal Blooms in a Shallow Fluvial Lake by Combining Hydrodynamic Modelling and Remote-Sensed Images. Water, 7(5): 1921-1942.

Prentice, M.J., Hamilton, D.P., Willis, A., O'Brien, K.R., Burford, M.A., 2019. Quantifying the role of organic phosphorus mineralisation on phytoplankton communities in a warm-monomictic lake. Inland Waters: 1-15.

Qin, B. et al., 2010. A drinking water crisis in Lake Taihu, China: linkage to climatic variability and lake management. Environ Manage, 45(1): 105-12. DOI:10.1007/s00267-009-9393-6

Qin, Q., Jian, S., 2017. The contribution of local and transport processes to phytoplankton biomass variability over different timescales in the Upper James River, Virginia. Estuarine Coastal & Shelf Science, 196: 123-133.

Qin, Y., Hu, S., 2018. Study on Release Characteristics and Recovery of Nitrogen and Phosphorus during the Anaerobic Fermentation of Excess Sludge, Iop Conference Series: Earth & Environmental Science.

Simiyu, B., Oduor, S., Rohrlack, T., Sitoki, L., Kurmayer, R., 2018. Microcystin Content in Phytoplankton and in Small Fish from Eutrophic Nyanza Gulf, Lake Victoria, Kenya. Toxins, 10(7): 275-.

Smagorinsky, J., 1963. General circulation experiments with the primitive equations. Monthly Weather Review, 91.

Smith, G.J., Daniels, V., 2018. Algal blooms of the 18th and 19th centuries. Toxicon, 142: 42-44.

Steffen, M.M. et al., 2017. Ecophysiological examination of the Lake Erie Microcystis bloom in 2014: linkages between biology and the water supply shutdown of Toledo, Ohio. Environmental Science & Technology, 51(12): acs.est.7b00856.

Walsby, A.E., Bleything, A., 1988. The Dimensions of Cyanobacterial Gas Vesicles in Relation to Their Efficiency in Providing Buoyancy and Withstanding Pressure. Microbiology, 134(10): 2635-2645.

Wang, C., Feng, T., Wang, P., Hou, J., Qian, J., 2017. Understanding the transport feature of bloom-forming Microcystis in a large shallow lake: A new combined hydrodynamic and spatially explicit agent-based modelling approach. Ecological Modelling, 343: 25-38. DOI:https://doi.org/10.1016/j.ecolmodel.2016.10.017

Wang, H. et al., 2016. Separation of wind's influence on harmful cyanobacterial blooms. Water Research, 98: 280-292.

Wang, J., Fu, Z., Qiao, H., Liu, F., 2019. Assessment of eutrophication and water quality in the estuarine area of Lake Wuli, Lake Taihu, China. Science of the Total Environment, 650.

Wang, J. et al., 2015. Effect of algal bloom on phosphorus exchange at the sediment–water interface in Meiliang Bay of Taihu Lake, China. Environmental Earth Sciences, 75(1): 57. DOI:10.1007/s12665-015-4810-z

WHO, 2011. WHO Guidelines for Drinking-Water Quality, fourth ed, WHO, Geneva,Switzerland.

Wurtsbaugh, W., 2015. Do Phosphorus and Nitrogen Act Synergistically to Exacerbate Algal Growth and Eutrophication.

Xue, Q.J. et al., 2018. Spatio-temporal variation of microcystins and its relationship to biotic and abiotic factors in Hongze Lake, China. J. Gt. Lakes Res., 44(2): 253-262. DOI:10.1016/j.jglr.2017.12.004

Yang, Z., Geng, L., Wang, W., Zhang, J., 2012. Combined effects of temperature, light intensity, and nitrogen concentration on the growth and polysaccharide content of Microcystis aeruginosa in batch culture. Biochemical Systematics and Ecology, 41: 130-135. DOI:https://doi.org/10.1016/j.bse.2011.12.015

Zeng, Q., Qin, L., Bao, L., Li, Y., Li, X., 2016. Critical nutrient thresholds needed to control eutrophication and synergistic interactions between phosphorus and different nitrogen sources. Environmental Science & Pollution Research International, 23(20): 1-12.

Zhao, C.S. et al., 2019. Quantitative assessment of the effects of human activities on phytoplankton communities in lakes and reservoirs. Sci Total Environ, 665: 213-225. DOI:10.1016/j.scitotenv.2019.02.117

Zhao, L. et al., 2013. Monthly Variation of Nitrogen and Phosphorus Volume in Taihu Lake, China. Journal of China Hydrology, 33(5): 28-1855.

Zhu, M. et al., 2013. Estimation of the algal-available phosphorus pool in sediments of a large, shallow eutrophic lake (Taihu, China) using profiled SMT fractional analysis. Environmental Pollution, 173(1): 216-223.

***Highlights (3 to 5 bullet points (maximum 85 characters including spaces per bullet point)**

Highlights:

- Algal input from upstream dominant the seasonal change of chl-a in Liangxi river
- In situ proliferation played an important role in algal vertical distribution
- Potential chl-a growth induced by excessive nutrient or temperature was quantified